BIOCHEMISTRY
including biophysical chemistry & molecular biology

Article

pubs.acs.org/biochemistry

Perturbing the General Base Residue Glu166 in the Active Site of Class A β-Lactamase Leads to Enhanced Carbapenem Binding and Acylation

Xuehua Pan,[†] Wai-Ting Wong,[†] Yunjiao He,[†] Yongwen Jiang,[‡] and Yanxiang Zhao*[,†]

[†]Department of Applied Biology and Chemical Technology, State Key Laboratory of Chirosciences, The Hong Kong Polytechnic University, Hung Hom, Kowloon, Hong Kong, P. R. China

[‡]State Key Laboratory of Bioorganic and National Products Chemistry, Shanghai Institute of Organic Chemistry, Chinese Academy of Sciences, 354 Fenglin Lu, Shanghai 200032, P. R. China

ABSTRACT: Most class A β-lactamases cannot hydrolyze carbapenem antibiotics effectively. The molecular mechanism of this catalytic inefficiency has been attributed to the unique stereochemistry of carbapenems, including their 6-α-hydroxyethyl side chain and the transition between two tautomeric states when bound at the active site. Previous studies have shown that the 6-α-hydroxyethyl side chain of carbapenems can interfere with catalysis by forming hydrogen bonds with the deacylation water molecule to reduce its nucleophilicity. Here our studies of a class A noncarbapenemase PenP demonstrate that substituting the general base residue Glu166 with Ser or other residues leads to a significant enhancement of the acylation kinetics by ∼100−500 times toward carbapenems like meropenem. The structures of PenP and Glu166Ser both in apo form and in complex with meropenem reveal that Glu166 is critical for the formation of a hydrogen bonding network within the active site that locks Asn170 in an orientation to impose steric clash with the 6-α-hydroxyethyl side chain of meropenem. The Glu166Ser substitution weakens this network and enables Asn170 to adopt an alternative conformation to avoid steric clash and accommodate faster acylation kinetics. Furthermore, the weakened hydrogen bonding network caused by the Glu166Ser substitution allows the 6-α-hydroxyethyl moiety to adopt a catalytically favorable orientation as seen in class A carbapenemases. In summary, our data identify a previously unreported role of the universally conserved general base residue Glu166 in impeding the proper binding of carbapenems by restricting their 6-α-hydroxyethyl group.

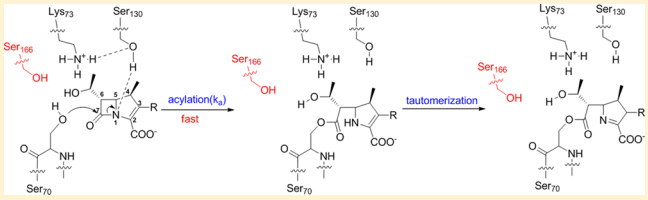

Carbapenems are a family of β-lactam antibiotics that is commonly referred to as a "last resort" defense against bacterial infection. Similar to other β-lactam antibiotics such as penicillins and cephalosporins, carbapenems bind and become irreversibly acylated to the active site of PBPs, which are responsible for bacterial cell wall synthesis.[1,2] This mechanism-based inhibition compromises the cell wall synthesis and leads to bacteria cell lysis. Notably, carbapenems show the broadest spectrum and highest potency against both Gram-positive and Gram-negative bacteria among all β-lactam antibiotics and are usually used as "last-line" treatment when other "front-line" antibiotics become ineffective because of antibiotic resistance.[1,2]

The production of β-lactamases is one of the major mechanisms for antibiotic resistance. These bacterial enzymes readily hydrolyze β-lactam antibiotics and render them inactive. Currently over 1000 β-lactamase enzymes and their derivatives have been identified. These enzymes are largely grouped into four classes (A−D) based on their sequences and catalytic mechanisms.[3,4] The widely disseminated and clinically significant class A β-lactamases are serine-based enzymes that use a catalytic residue Ser70 (numbered according to Ambler position)[5] for β-lactam hydrolysis. The hydrolytic process includes two steps, that is, the initial acylation step in which the catalytic Ser70 attacks the amide bond of the β-lactam substrate and forms an acyl−enzyme covalent intermediate and the subsequent deacylation step in which the acyl adduct is hydrolyzed by a deacylation water molecule, and the antibiotic with its β-lactam ring opened is released as an inactivated product.[6,7] The rate of this catalysis is usually very fast for naturally good substrates such as penicillin and first-generation cephalosporins, with k_{cat}/K_m approaching the diffusion limit of $\sim 10^8$ M^{-1} s^{-1}.

While the catalytic machinery of class A β-lactamases is highly effective in hydrolyzing penicillins and cephalosporins, it turns over carbapenems rather poorly. The reaction scheme of carbapenem is largely similar to that of other β-lactam antibiotics. For the acylation step, residues Glu166 and Lys73 share the role of the general base in either a competitive or cooperative manner to activate the Ser70 hydroxyl side chain for its nucleophilic attack on the β-lactam amide bond. This attack leads to the formation of the acyl adduct in which the β-lactam ring is opened and covalently linked to Ser70 (Figure 1).[1−4,7,8] At the deacylation step, Glu166 is the exclusive general base used to activate the deacylation water molecule for

Received: December 3, 2013
Revised: June 25, 2014
Published: July 14, 2014

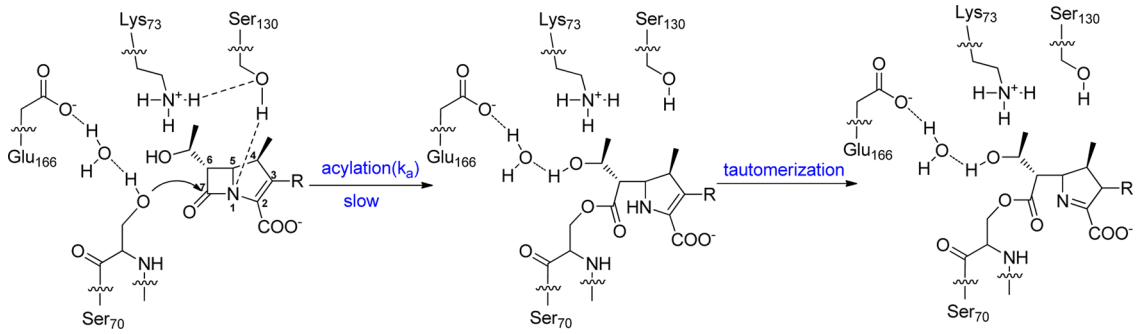

Figure 1. Summary of the slow acylation and tautomerization of carbapenems by class A β-lactamase. The enzyme−substrate acyl adduct after tautomerization is highly stable and undergoes little subsequent deacylation. The dashed lines mark the H-bonds.

its hydrolytic attack on the acyl adduct. The hydrolyzed product, no longer active as an antibiotic, is subsequently released from the active site and Ser70 is regenerated.[1−4,7,8] However, the acylation rate for carbapenems is generally slow and the deacylation activity is almost nonexistent. In fact, carbapenems can even serve as inhibitors for class A β-lactamases because of the extreme stability of the acyl−enzyme adduct. Extensive structural studies have identified two distinct stereochemistry features of carbapenems that are critical for their catalytic inefficiency.[1−3] First of all, carbapenems, such as the meropenem used in our study, contain a 6-α-hydroxyethyl group at the C6 position of the β-lactam nucleus (Figure 1) while penicillins and cephalosporins contain a 6-β-acylamino side chain. This hydroxyethyl side chain has been shown to cause a steric clash with residues within the active site to impede acylation or to form H-bonds with the deacylation water molecule to weaken its nucleophilicity and interfere with deacylation.[9,10] Additionally, the pyrroline moiety of carbapenems has been shown to undergo tautomerization and convert from the catalytically competent Δ^2 conformation to the catalytically incompetent Δ^1 conformation when bound at the active site of class A β-lactamases with a slow turnover rate (Figure 1).[9−12] Lastly, the presence of the carbon atom at the C-4 position in carbapenems instead of the sulfur atom in penicillins and cephalosporins has been argued to contribute to their resistance to β-lactamase hydrolysis.[1]

Alarmingly, some class A β-lactamases with carbapenemase activity have emerged in recent years. These enzymes, such as the GES, SFC, and KPC series, have acquired an improved kinetic profile toward carbapenems through the evolutionary substitution of amino acid residues at certain strategic positions while they have retained an active site that is largely similar to that of a noncarbapenemase.[13−16] The exact molecular mechanism of how such substitutions lead to enhanced catalytic activity toward carbapenems is not fully understood. Some substitutions, such as Asn170Gly/Ser seen in the GES series, are believed to allow better coordination of the deacylation water molecule for effective deacylation.[12,17−19] Other substitutions, such as Arg244Ala and Ala237Thr in the KPC series, likely select the Δ^2 tautomeric state over the Δ^1 state.[20,21] For the most notable substitutions of Ala69Cys and Ala238Cys that are seen in all class A carbapenemases, little is known about how these substitutions enhance carbapenem hydrolysis, although structural studies reveal that these two substitutions lead to the formation of a disulfide bond close to the catalytic Ser70 residue and slightly alter the overall shape of the active site.[22]

Here we present our work to delineate the role of the general base residue Glu166 in carbapenem binding and acylation. Previous studies have reported multiple orientations of the hydroxyethyl side chain when carbapenems are bound at the active site, yet the factors that determine such orientations and their functional relevance are not well characterized. Here, our kinetics studies and crystal structures reveal that the universally conserved general base residue Glu166 exerts a significant impact on the proper orientation of the hydroxyethyl side chain, and consequently, plays a critical role in the binding and acylation of carbapenems to the active site of class A β-lactamases.

EXPERIMENTAL PROCEDURES

Protein Expression and Purification. Wild-type PenP was subcloned into a modified PET 30a vector containing an N-terminal His6 tag and the HRV 3C protease cleavage site. Substitutions of Glu166 to different amino acids including Ser, Gln, His, Tyr, and Trp were done by site-directed mutagenesis.

The same expression and purification protocol was employed for wild-type and all of the mutants. Specifically, the recombinant plasmids were transformed into the *E. coli* strains BL21(DE3), and the desired bacteria colony was selected by using a kanamycin-containing agar plate. Then one single colony was picked and inoculated in 50 mL of LB media and grown at 37 °C overnight. Subsequently, the overnight bacteria culture was diluted 100 fold into 2.4 L of LB media with 30 μg/mL of kanamycin and was incubated at 37 °C until the OD_{600} reached 0.6−0.8. Protein expression was induced by adding IPTG at the final concentration of 500 μM, and the cell was grown at 30 °C for an additional 5 h and was collected by centrifugation at 5000 rpm for 15 min at 4 °C.

In the purification step, the cell pellet was resuspended with a lysis buffer composed of 50 mM Tris and 150 mM NaCl, with pH 8.0, plus freshly added 1 mM phenylmethanesulfonyl fluoride and 10 mM of beta-mecaptoethanol, and then was disrupted by sonication. The soluble fraction obtained by ultracentrifugation was loaded onto the HisTrap affinity column (GE Healthcare) and then was washed with 200 mL of His-binding buffer (20 mM sodium phosphate, 500 mM NaCl, 40 mM imidazole, pH 7.4). The bound protein was eluted with His-elution buffer (20 mM sodium phosphate, 500 mM NaCl, 500 mM imidazole, pH 7.4). Then the His-tag was cleaved by incubating the elution fraction with HRV 3C protease at 4 °C for overnight, and the mixture was reloaded into the HisTrap affinity column to remove the tag. Finally, the tag-free protein was further purified by gel filtration using HiLoad 16/60, superdex 75 prep grade (GE Healthcare).

dx.doi.org/10.1021/bi401609h | *Biochemistry* 2014, 53, 5414−5423

Table 1

	E166S	E166S + cephaloridine	E166S + meropenem
Data Collection			
space group	P1	P1	P21
unit cell parameters			
a, *b*, *c* (Å)	43.31, 46.19, 66.28	43.37, 45.80, 66.12	43.26, 90.96, 66.20
α, *β*, *γ* (deg)	78.43, 75.71, 69.36	77.85, 75.41, 69.00	90.00, 104.24, 90.00
resolution range (Å)	42.88−1.93 (2.03−1.93)	42.38−1.93 (2.03−1.93)	45.48−2.30 (2.42−2.30)
no. of total reflns	124 601	124 292	157 513
no. of unique reflns	32 459	31 762	22 157
I/σ	10.5(5.2)	11.5(4.8)	19.0(10.6)
completeness (%)	92.8(87.2)	92.0(87.1)	100(100)
R_{merge} (%)	8.3(18.2)	8.1(21.1)	7.3(15.5)
Structure Refinement			
resolution (Å)	42.88−1.93	39.73−1.93	38.11−2.30
R_{cryst}/R_{free} (%)	17.7/23.1	17.6/22.9	18.1/24.2
RMSD-bonds (Å)/angles (deg)	0.018/1.909	0.018/1.980	0.015/2.045
no. of reflns			
working set	30 806	30 137	20 988
test set	1648	1617	1131
no. of atoms			
protein atoms	4104	4109	4104
ligand/ion atoms		44	52
water molecules	425	411	314
average *B*-factor (Å^2)			
main chain	14.214	13.396	12.471
side chain	18.538	17.370	16.192

ESI-MS and UV−vis Spectrophotometry Measurements for Enzyme Kinetics. The catalytic parameters used to derive k_{cat}/K_m values were measured using the UV−vis spectrophotometry method. The detailed procedure was reported previously.[23] The acylation kinetics for the enzyme and substrate were measured by ESI-MS and the detailed procedure has been reported in our previous studies.[23−25] The brief procedure proceeded as follows, the enzyme−substrate binding interaction was initiated by the mixing of 35 μL of the 5 μM enzyme (wild-type, Glu166Ser, Glu166Gln, Glu166His, Glu166Tyr, Glu166Trp) in 20 mM ammonium acetate (pH 7.0) with 35 μL of 10 uM substrate (meropenem and imipenem) in the same buffer. At desired time intervals, the reaction was quenched by the addition of 70 μL of 1% formic acid (v/v) in acetonitrile either manually for wild-type PenP or by the quench−flow apparatus (Biologic SFM-400/Q) for the mutants because of their fast kinetics. The resulting solution was characterized by mass spectrometry. Normally, there are two major peaks in the mass spectrum, one for the enzyme itself (E) and the other for the acyl-adduct (ES*). The relative concentration of free enzyme ([E]) and the acyl-adduct ([ES*]) can be determined by the integration of the area under the measurement of the intensity of these two peaks, while the total amount of enzyme ($[E_{total}]$) can be calculated from the sum of [E] and [ES*] ($[E_{total}] = [E] + [ES^*]$). The obtained value of $[ES^*]/[E_{total}]$ was plotted as a function of the duration time (t) with eq 1:

$$[ES^*]/[E_{total}] = B[1 - \exp(-k_a t)] \quad (1)$$

In this equation, k_a is the acylation constant and B represents the relative concentration of ES in the steady state. Considering the fast kinetics of these mutants and the low initial concentration of the substrate [S], the second-order rate constants for the acylation reaction can be approximated with eq 2:

$$k_a/[S] = k_2/K_d = k_{cat}/K_m \quad (2)$$

Crystallization and Structure Determination. The crystals of PenP Glu166Ser were grown at 16 °C by the hanging drop vapor diffusion method. One μL of protein solution in a buffer of 20 mM Tris, 50 mM NaCl, pH 7.5 was mixed with 1 μL of reservoir buffer, which was composed of 0.1 M Tris, pH 8.0, 22.5% PEG3350, and 0.4 M ammonium acetate. Crystals appeared after 4−5 days and were harvested after they had grown to ∼100 μm in size. Cephaloridine and meropenem were soaked into the crystals by incubating the Glu166Ser apo crystals in a reservoir buffer containing 0.01 M cephaloridine and saturated meropenem for 7 and 25 min, respectively. The crystals were cryoprotected in reservoir solution plus 20% ethylene glycol for 1 min before they were mounted to the in-house Rigaku MicroMaxTM-007HF X-ray machine for data collection. Diffraction data were collected at 100 K, integrated by Mosflm,[26] and scaled by the SCALA module[27] in CCP4. All of the structures were solved by molecular replacement using the PHASER module in the CCP4i suite of programs with the PenP wild-type structure (PDB ID: 4BLM) as a search model.[28] The subsequent structural refinement was conducted using the REFMAC module in CCP4.[29] Manual structure rebuilding was done using WINCOOT.[30] Data collection and refinement statistics are summarized in Table 1. The coordinates of Glu166Ser structures were deposited into the Protein Data Bank (PDB ID: 4N92 for the apo Glu166Ser structure, 4N9K for the Glu166Ser−cephaloridine structure, and 4N9L for the Glu166Ser−meropenem structure). The structure figures were prepared using the CCP4MG package[31] in CCP4.

dx.doi.org/10.1021/bi401609h | *Biochemistry* 2014, 53, 5414−5423

(a)

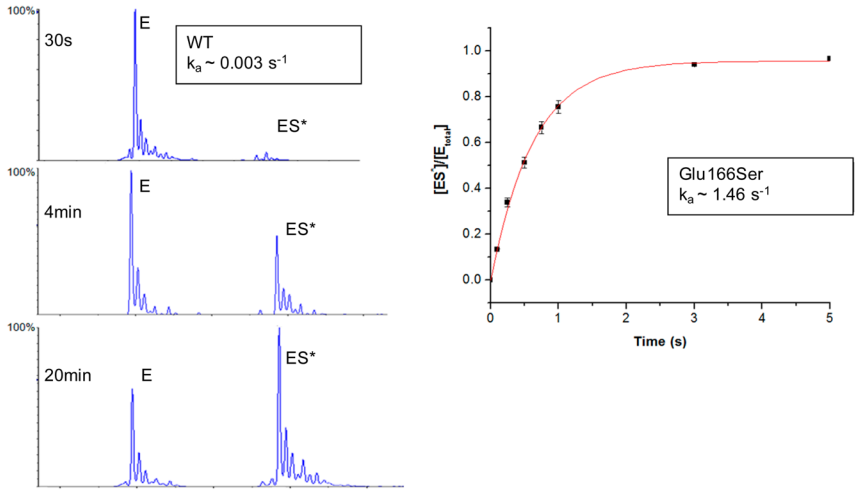

(b)

Construct	Cephaloridine (k_{cat}/K_m)	Cephaloridine (k_a/[S])	Meropenem (k_a/[S])	Imipenem (k_a/[S])
WT	0.40 ±0.02 ($s^{-1}\mu M^{-1}$)	> 2.0 ($s^{-1}\mu M^{-1}$)	0.32±0.04 ($s^{-1}mM^{-1}$)	ND
Glu166Ser	0.001±0.0004 ($s^{-1}\mu M^{-1}$)	> 2.0 ($s^{-1}\mu M^{-1}$)	146±6 ($s^{-1}mM^{-1}$)	84±4 ($s^{-1}mM^{-1}$)
Glu166Gln	ND	> 2.0 ($s^{-1}\mu M^{-1}$)	34±5 ($s^{-1}mM^{-1}$)	20±2 ($s^{-1}mM^{-1}$)
Glu166Trp	ND	> 2.0 ($s^{-1}\mu M^{-1}$)	39±2 ($s^{-1}mM^{-1}$)	22±2 ($s^{-1}mM^{-1}$)

(c)

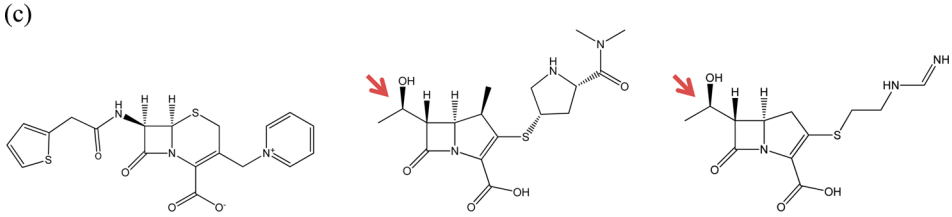

Figure 2. Enhanced acylation rate for carbapenems upon substitution of Glu166. (a) Time-dependent profile of meropenem acyl adduct formation for both wild-type PenP (left) and Glu166Ser substitution (right). (b) The second order reaction rate k_{cat}/K_m or the acylation rate k_a/[S] for different PenP substitutions with cephaloridine, meropenem, and imipenem as the substrates. The derivation of k_a/[S] as second-order rate constant is described in the experimental procedure (ND, not detectable). (c) Chemical structures of the three substrates used in panel b. The arrows mark the hydroxyethyl group that is unique to carbapenems.

RESULTS

Our biochemical and structural studies were conducted using β-lactamase PenP from *Bacillus licheniformis*. PenP shares >80% of its sequence identity with the clinically significant TEM and SHV β-lactamases. Our previous studies have demonstrated that the kinetic profile of PenP is representative of a narrow-spectrum class A β-lactamase.[25] It can readily hydrolyze penicillins and first-generation cephalosporins such as cephaloridine with k_{cat}/K_m approaching 10^6 M^{-1} s^{-1}. For second-generation cephalosporins, such as cefuroxime, its kinetics are about 3 orders of magnitude slower with k_{cat}/K_m at ~10^3 M^{-1} s^{-1}. Because of its thermal stability (T_m ≈ 50 °C), PenP is significantly more amenable to mutations and structural studies than are TEM and SHV series.[24,25] Thus, PenP is used in our studies as a model system for class A β-lactamases.

Substitution of the General Base Residue Glu166 Leads to Enhanced Acylation of Carbapenem. We first investigated whether PenP would have any carbapenemase activity. Meropenem, as the representative carbapenem substrate, was added to PenP at a 10 μM concentration and a 2:1 molar ratio. The time-dependent profile of ES* formation as tracked by ESI-MS is shown in Figure 2a. The second-order acylation rate (k_a) as measured from this profile is about 0.3 s^{-1} mM^{-1}, about 3−5 orders of magnitude slower than the acylation kinetics of penicillins and cephalosporins (Figure 2b).[25] The ES* adduct formed in PenP is extremely stable, and no deacylation could be detected by ESI-MS even after 30 h. For imipenem, almost no acylation activity could be detected even after 24 h, let alone the subsequent deacylation (Figure 2b). These data confirm that PenP is a class A non-carbapenemase with an extremely slow acylation rate and no detectable deacylation activity.

To probe the role of Glu166 in the slow binding and acylation kinetics for meropenem, this residue was substituted

dx.doi.org/10.1021/bi401609h | *Biochemistry* 2014, 53, 5414−5423

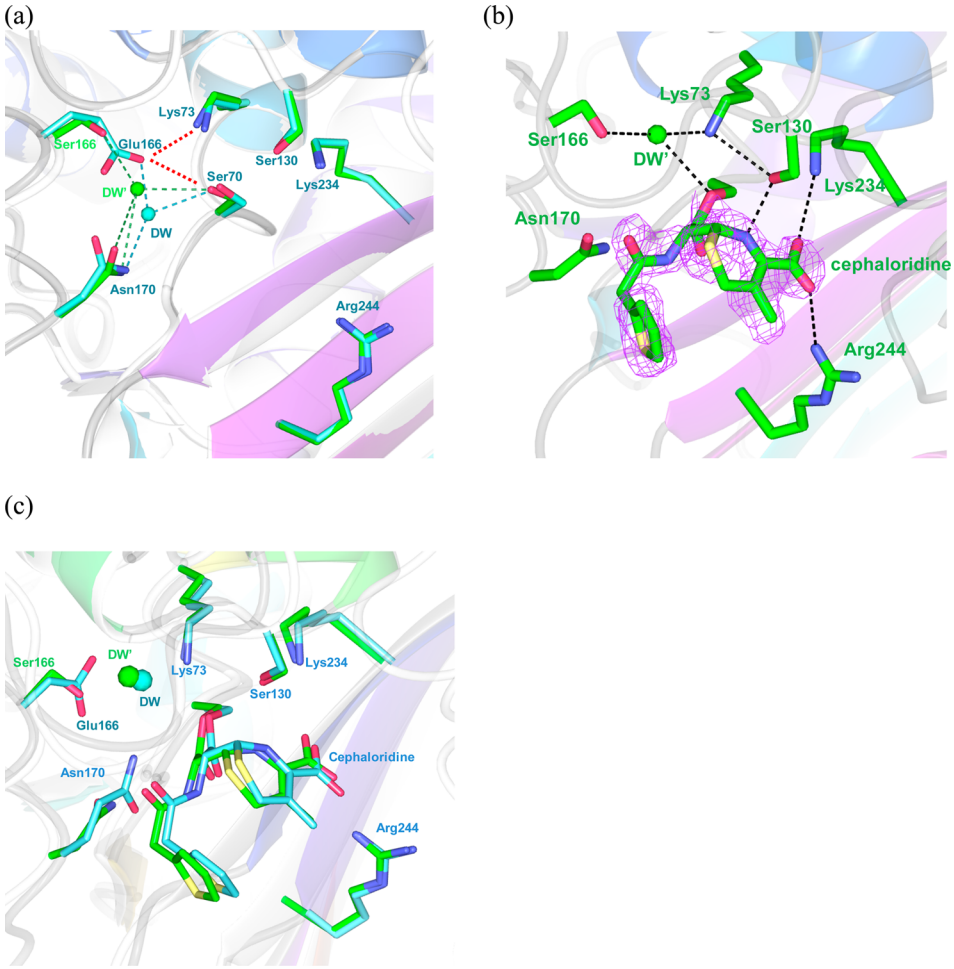

Figure 3. The active site of Glu166Ser is acylation-competent and deacylation-impaired toward cephaloridine. (a) The active site of Glu166Ser is superimposed with that of the wild-type. Key residues for catalysis and the deacylation water are shown for wild-type (DW, cyan) and Glu166Ser (DW′, green). The two sets of dashed lines indicate the H-bonding network between the deacylation water and other active site residues. (b) The active site of Glu166Ser with cephaloridine acylated to Ser70. Cephaloridine is drawn in a bond-and-stick model. A simulated annealing $2F_o - F_c$ composite omit map (purple) around cephaloridine is drawn in a mesh format contoured at 1.5 σ. The dashed lines indicate the H-bonds between cephaloridine and the active site residues. (c) The Glu166Ser−cephaloridine (green) acyl adduct structure is superimposed with that of PC-1 (PDB ID: 1GHM) (cyan). The two structures are largely identical, even the two deacylation waters are in close proximity.

by Ser, Gln, and Trp to replace the carboxylate side chain of Glu166 with a smaller hydroxyl group (Glu166Ser), a polar side chain of the same size (Glu166Gln), and a large hydrophobic side chain (Glu166Trp). These substitutions were expected to abolish deacylation since the exclusive general base for deacylation, that is, Glu166, would be lost. However, these mutations were not expected to affect acylation since the alternative general base, that is, Lys73, can still activate the catalytic Ser70[24,25] and facilitate its nucleophilic attack on meropenem and subsequent acyl adduct formation. All of these substituted mutant proteins were purified and their kinetics profiles toward carbapenems were characterized under the same setup as described above for the wild-type enzyme.

Unexpectedly, the acylation rate as measured by ESI-MS showed a significant enhancement for all of the substituted mutants (Figure 2a,b). For meropenem, the second-order acylation rate ($k_a/[S]$) of Glu166Ser is ∼146 s^{-1} mM^{-1}, nearly 500 times faster than that of the wild-type. The acylation rate of Glu166Gln is ∼34 s^{-1} mM^{-1}, about 100 times faster than that of the wild-type. Even the Glu166Trp substitution showed ∼100 times faster acylation rate at ∼39 s^{-1} mM^{-1} than did the wild-type. A comparable trend of enhancement was also observed for imipenem, another clinically used carbapenem antibiotic. The binding and acylation of imipenem to wild-type PenP was almost nondetectable, yet the three substitutions showed second-order acylation rates in the range of 20−80 s^{-1} mM^{-1}, comparable to that of meropenem and significantly improved over the wild-type. Furthermore, these Glu166 substitutions had little effect on the fast acylation rate of cephaloridine, the good substrate. Their second-order acylation rates toward cephaloridine are similar to that of the wild-type and are too fast to be measured by the ESI-MS method. Instead, the k_{cat}/K_m value of the wild-type PenP (>2 s^{-1} μM^{-1}), as reported in our previous work,[24,25] was used as a reference for these mutants (Figure 2b).

In summary, the Ser, Gln, and Trp substitutions at Glu166 lead to a significant enhancement in the acylation rate by ∼100−500 times, specifically for carbapenems. At this rate, the velocity of carbapenem acylation is comparable to that for penicillins and cephalosporins. No enhancement in the deacylation step of carbapenems was detected for any of these substitutions, probably due to the extremely low deacylation activity in the wild-type PenP enzyme as well as

dx.doi.org/10.1021/bi401609h | *Biochemistry* 2014, 53, 5414−5423

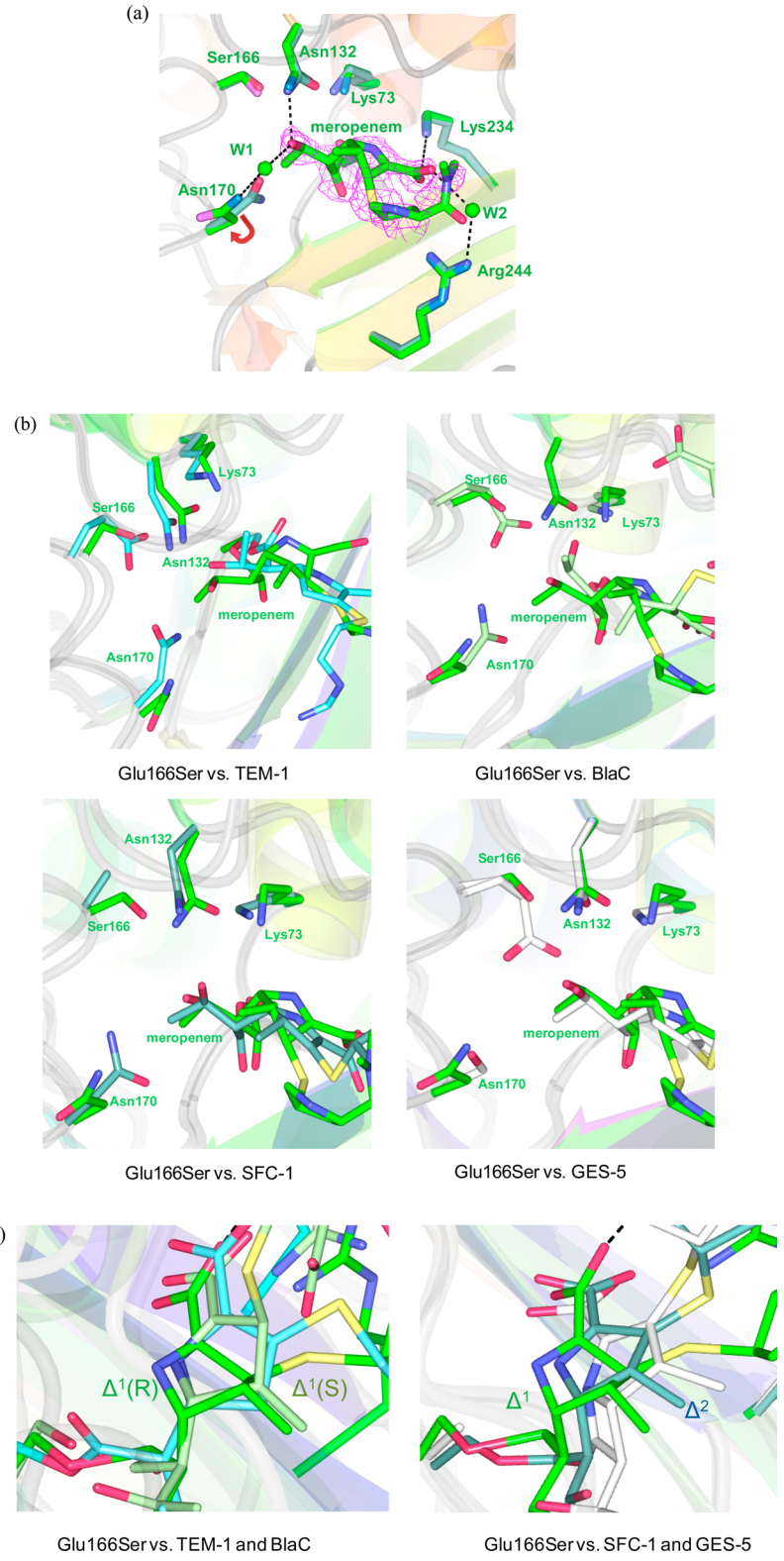

Figure 4. Structure of Glu166Ser in complex with meropenem shows a distinct binding mode. (a) The structure of Glu166Ser with meropenem acylated to Ser70 (green) is superimposed with the Glu166Ser apo structure (cyan). Key residues at the active site and meropenem are drawn in a bond-and-stick model. The simulated annealing $2F_o - F_c$ composite omit map (purple) around meropenem is drawn in a mesh format contoured at 1.2 σ. The interactions of meropenem with the active site residues are marked by dashed lines. The arrow marks the "flip out" of the Asn170 side chain as compared to that seen in the wild-type structure. (b) Superposition of the Glu166Ser–meropenem structure with four class A β-lactamases, including TEM-1, in complex with imipenem (PDB ID: 1BT5), BlaC in complex with ertrapenem (PDB ID: 3M6H), SFC-1 in complex with imipenem (PDB ID: 4EV4), and GES-5 in complex with imipenem (PDB ID: 4H8R) to compare the orientation of the hydroxyethyl group and the tautomeric state of meropenem. (c) Superposition of the Glu166Ser–meropenem structure with the same four structures in panel b but grouped into 2 tautomeric states for better illustration, including the Δ^1 state as seen in class A noncarbapenemases TEM-1 and BlaC and the Δ^2 state as seen in class A carbapenemases SFC-1 and GES-5.

dx.doi.org/10.1021/bi401609h | *Biochemistry* 2014, 53, 5414–5423

the loss of the general base Glu166 for deacylation in the substituted mutants.

Glu166Ser Structure and Its Complex with Cephaloridine Reveal an Active Site That Is Acylation-Competent and Deacylation-Deficient. To determine the molecular mechanism of enhanced acylation toward carbapenems in the substituted mutants, we chose to determine the structure of PenP with the Glu166Ser substitution because of its fastest acylation rate. The PenP Glu166Ser apo structure was solved at the resolution of 1.93 Å to investigate whether Glu166Ser leads to any significant structural change within the active site.

The Glu166Ser apo structure is largely identical to that of the wild-type enzyme (PDB ID: 4BLM), with an overall RMSD value of only ∼0.23 Å. The active site of Glu166Ser shows little difference to that of the wild-type (Figure 3a). The key catalytic residues such as Ser70, Lys73, Ser130, Asn170, Lys234, and Arg244 all show identical conformations in these two structures. The Glu166Ser substitution extends its side chain hydroxyl group in the same orientation as the carboxylate group of Glu166 in the wild-type structure. Even the position of the respective deacylation water molecule is fairly similar between these two structures, with a shift of only 1.2 Å. In both the Glu166Ser and wild-type structure, the deacylation water molecule forms an extensive H-bond network with Oγ of Ser166, Oγ of Ser70, and Oδ1 and Nδ2 of Asn170. Notably, Ser166 has no H-bonding interaction with either Ser70 or Lys73 because of its smaller size, while in the wild-type structure, Glu166 is within 3.5 Å from both residues to form potential H-bond interactions.

We then proceeded to solve the structure of Glu166Ser in complex with cephaloridine, the good substrate. While our kinetic studies have shown that Glu166Ser substitution specifically enhances the acylation rate of carbapenems but does not affect the acylation rate of cephaloridine, we aim to compare the acyl adduct structure of Glu166Ser in complex with cephaloridine to that with meropenem to delineate the structural factors that contribute to this substrate-specific enhancement.

The Glu166Ser−cephaloridine structure reveals the acyl adduct complex with cephaloridine covalently linked to Ser70. Overall, the structure of the Glu166Ser−cephaloridine acyl complex is nearly identical to that of the Glu166Ser apo structure with an overall RMSD value of only ∼0.18 Å. The simulated annealing $2F_o - F_c$ composite omit map clearly shows the presence of cephaloridine with its β-lactam carbonyl covalently linked to the Oγ of Ser70 to form a stable acyl−enzyme adduct (Figure 3b). The binding mode of cephaloridine is nearly identical to that seen in another class A β-lactamase, PC1 (Figure 3c).[32] The carbonyl of the acylated cephaloridine is positioned in the oxyanion hole formed by the amide of Ser70 and Ala237. The pyridine group at the R1 position extends across the active site with the terminal carboxylate forming H-bonds with Thr235 and Arg244. The thiophene group at the R2 position projects toward the solvent with a H-bond between its amino group and the carbonyl of Ala237. A putative deacylation water molecule is located within the active site as a site almost identical to that seen in the wild-type enzyme and it forms H-bonds with Oγ of Ser166, Oγ of Ser70, and Nζ of Lys73 (Figure 3c). Yet in the absence of a general base, this deacylation water molecule cannot be activated to carry out a nucleophilic attack on the ester bond of the acylated substrate for deacylation. In summary, the Glu166Ser substitution causes little structural change at the active site and renders the enzyme acylation-competent and deacylation-deficient.

Structure of Glu166Ser in Complex with Meropenem Shows a Distinct Binding Mode for Meropenem. To understand the molecular mechanism of the enhanced acylation kinetics caused by Glu166Ser substitution, the structure of the Glu166Ser−meropenem acyl complex was determined at a 2.3 Å resolution. The overall structure of Glu166Ser in complex with meropenem is nearly identical to that of Glu166Ser with an overall RMSD value of only ∼0.21 Å. The simulated annealing $2F_o - F_c$ composite omit map clearly shows the presence of meropenem at the active site, covalently linked to the Ser70 side chain (Figure 4a). The electron density map is of sufficient quality that the entire molecule of meropenem can be traced except for the dimethylamino group at the very end.

The binding mode of meropenem at the active site has several features that resemble those that have been reported for class A carbapenemases. First, the β-lactam carbonyl of meropenem is located in the oxyanion hole formed by the amide groups of Ser70 and Ala237 (Figure 4a). This orientation is the same as those seen in BlaC, SFC-1, and GES-5.[10−12] In contrast, this carbonyl has been reported to flip out of the oxyanion hole in the TEM-1 structure and adopt a catalytically incompetent conformation to inhibit this class A non-carbapenemase.[9]

In addition to the carbonyl similarity, the hydroxyethyl side chain also adopts an orientation similar to that seen in SFC-1 and GES-5 carbapenemases[11,12] (Figure 4b). Three alternative rotamer conformations of this hydroxyethyl side chain, rotated 120° relative to each other by the dihedral angel, have been reported in the literature.[9−12] In the two distinct rotamers observed in class A noncarbapenemases, TEM-1 and BlaC, the hydroxyl moiety within the hydroxyethyl side chain is oriented toward Glu166 and forms H-bonds with both the Oγ of Glu166 and the putative deacylation water. Such interactions have been speculated to reduce the basicity of Glu166 and the nucleophilicity of the deacylation water, thus impeding deacylation (Figure 4b). In our Glu166Ser structure as well as in the structures of class A carbapenemases SFC-1 and GES-5, the hydroxyl group extends toward the solvent and forms H-bonds with Nδ2 of Asn132 and a solvent water molecule (Figure 4b). This orientation is speculated to be beneficial for deacylation as its interaction with Glu166 or the deacylation water molecule is lost. In our Glu166Ser structure, no deacylation water is clearly visible in the active site, probably because of the absence of a general base residue. Instead, a piece of spherically-shaped electron density is found near the Ser166 side chain. This object is clearly visible in both copies of the PenP molecules in the asymmetric unit, even at the high contour level for both the $F_o - F_c$ and $2F_o - F_c$ maps (data not shown). Considering the nearby Lys73 residue is most likely in its protonated state, we speculate that the spherical piece of electron density represents an anion, probably chloride, as it is used in our buffer solutions.

While the hydroxyethyl side chain adopts a conformation seen in carbapenemases, the pyrroline ring of the acylated meropenem clearly adopts the Δ^1 tautomeric state, which is the same as seen in noncarbapenemases TEM-1 and BlaC[9,10] (Figure 4c). The CN bond is sp2 hybridized with the colinearization of N1, C2, C3, and C5. The carboxylate of the pyrroline ring forms H-bonds with Oγ1 of Thr235, Nη1 of Arg244, and a tautomeric water molecule. In contrast to the class A carbapenemases SFC-1, GES-1, and GES-5, the

dx.doi.org/10.1021/bi401609h | Biochemistry 2014, 53, 5414−5423

pyrroline ring adopts the Δ^2 tautomer with the CN bond in sp3 hybridization and the colinearization of N1, C2, C3, and C4.[11,12] Closer inspection reveals that the newly formed chiral center C3 adopts the *R* configuration. The thioethyl sulfur atom rises significantly above the plane defined by atoms C2, C3, and C4. The angle formed by the C3−S bond and this plane is ∼50° (Figure 4c). This orientation of the pyrroline ring is similar to that seen in the class D OXA-1 structure (Δ^1 tautomer in *R* configuration), while it is distinctively different from those in class A carbapenemases SFC-1 and GES-5 (Δ^2 tautomer) or class A noncarbapenemases (Δ^1 tautomer in *S* configuration).[33]

In summary, our Glu166Ser structure shows a distinct binding mode of meropenem that mixes features of carbapenem structures when bound in the active site of either carbapenemases or noncarbapenemases. Its hydroxyethyl group adopts a conformation seen in class A carbapenemases, while its pyrroline ring adopts the Δ^1 tautomeric state seen in noncarbapenemases but with an *R* configuration instead of *S*. Such a "hybrid" binding mode has not been reported before and likely reflects the conformational flexibility of meropenem within the acyl−enzyme complex.

DISCUSSIONS

Residue Glu166 is critical in the catalysis of β-lactam antibiotics by class A β-lactamases. It serves as the exclusive general base in the deacylation step to activate a water molecule for its hydrolytic attack on the acyl−enzyme adduct. Extensive studies have shown that a mutation of Glu166 leads to almost a complete loss of the deacylation activity, although acylation is hardly affected. Additionally, Glu166 forms extensive H-bonding interactions with several key elements at the active site, including the catalytic Ser70 and the alternative general base residues Lys73 and Asn170. These interactions are essential in defining the local electrostatic environment and structural plasticity within the active site to facilitate substrate binding and catalysis. Yet little is reported on how this H-bonding capacity of Glu166 may impact the kinetic properties of class A β-lactamases toward diverse substrates.

Here our kinetic study shows that, for a narrow-spectrum class A β-lactamase that has an intrinsicly low binding affinity and slow acylation rate of carbapenems, substituting Glu166 with residues such as Ser, Gln, and Trp greatly enhances the acylation rate by ∼100−500 times. This enhancement is specific for carbapenems, since the fast acylation rate for good substrates like cephaloridine is little affected by these Glu166 residues. Furthermore, the enhancement effect from these Glu166 substitutions is not likely due to simple size effect since even the substitution of Trp with its bulky side chain can lead to a significant enhancement.

Our structural studies of Glu166Ser in complex with both cephaloridine and meropenem reveal that the Glu166Ser substitution leads to an altered pattern of H-bonding interactions within the active site that renders the binding of meropenem more favorable, while it exerts little effect on cephaloridine binding.

One change that is favorable for meropenem binding as a result of the Glu166Ser substitution is the alternative conformation of the Asn170 side chain. In the acyl adduct structure of Glu166Ser in complex with meropenem, this side chain rotates away from the active site and avoids a steric clash with the hydroxyethyl group (Figure 4a). In the Glu166Ser apo structure, as well as in most published structures of class A β-lactamases, the Asn170 side chain adopts a rotamer conformation that forms stable H-bonds with the deacylation water. This conformation is further strengthened by Glu166 as its carboxylate side chain forms a strong H-bond with the deacylation water molecule and coordinates a H-bonding network involving the deacylation water molecule, Asn170, and itself. The Glu166Ser substitution weakens this H-bonding network significantly. As a result, the deacylation water is absent and the Asn170 side chain flips out to accommodate the hydroxyethyl group of meropenem for more efficient binding and acylation. In this aspect, Glu166 enforces a H-bonding network at the active site to impose a steric clash with meropenem and impede its binding and acylation.

The second favorable change is the proper orientation of the hydroxyethyl side chain within the active site upon the Glu166Ser substitution. By comparing the different rotamers of this side chain in the structures of noncarbapenemases like TEM-1 and BlaC, as well as carbapenemases like SFC-1 and GES-5, it appears that Glu166, with its carboxylate side chain, effectively "pulls" in the hydroxyl group within the hydroxyethyl moiety for favorable H-bonding interactions. Such preference, however, weakens the basicity of this general base residue and the nucleophilicity of the nearby deacylation water molecule. Upon Glu166Ser substitution, this pulling force is reduced and the hydroxyl group adopts the thermodynamically preferred orientation with the hydroxyl group oriented toward the solvent to facilitate proper hydrolysis. Indeed, this orientation of meropenem in our Glu166Ser structure has also been observed in structures of carbapenemases like GES-5 and SFC-1.

Lastly, while Glu166 exerts a strong influence on the interactions between the active site residues and the unique hydroxyethyl moiety of carbapenems, it does not appear to exert a direct influence on the tautomeric state of the acylated carbapenem. Instead, residues at positions 130, 235, and 244 play exclusive roles in determining the tautomer state of the bound meropenem by coordinating a set of H-bonds with the terminal carboxylate of the carbapenems. For PenP, Arg244 is located about ∼4.4 Å away from the carboxylate of meropenem, thus unable to form a strong H-bond. Furthermore, no water molecule can be found in between Arg244 and the carboxylate to forge strong H-bonds. Such an absence of tautomeric H-bonds could have contributed to the carbapenem substrate adopting the Δ^1 tautomeric state in the *R* configuration.

In summary, our studies uncover a previously unreported role of Glu166 in impeding carbapenem catalysis. Through an extensive H-bonding network, this general base residue can strongly influence the binding of carbapenems by mediating their interactions with the active site. Either by coordinating Asn170 to impose a steric clash with carbapenems or by pulling in the hydroxyethyl group of carbapenems and interfering with deacylation, Glu166 can impede the binding and acylation of carbapenems. Such impediment is not observed for good substrates like cephaloridine because they do not contain the hydroxyl moiety that is unique for carbapenems. Thus, the H-bonding interactions between Glu166 and the unique hydroxyethyl moiety of carbapenems, either direct or through Asn170, play a major role in impeding the binding and acylation of carbapenems. Residue substitutions like Asn170Ser, observed in GES family of carbapenemases, probably circumvent this impedance to enhance hydrolytic activity toward carbapenems.

dx.doi.org/10.1021/bi401609h | *Biochemistry* 2014, 53, 5414−5423

AUTHOR INFORMATION

Corresponding Author

*E-mail: yanxiang.zhao@polyu.edu.hk, phone: 852-34008706.

Funding

This work was supported by the Research Grants Council Grants No. PolyU5639/09M, PolyU5644/10M, PolyU 5640/11M, HKUST6/CRF/10, and AoE/M-09/12. Funding support from the Research Committee of the Hong Kong Polytechnic University is also acknowledged.

Notes

The authors declare no competing financial interest.

ACKNOWLEDGMENTS

Former lab members Fengyi Tang and Roderick Dirkswager are acknowledged for their technical support.

ABBREVIATIONS

ESI-MS, electrospray ionization mass spectrometry; H-bonds, hydrogen bonds; HRV, human rhinovirus; IPTG, isopropyl β-D-1-thiogalactopyranoside; LB, lysogeny broth; OD, optical density; PBP, penicillin binding protein; RMSD, root−mean−square deviation

REFERENCES

(1) Papp-Wallace, K. M., Endimiani, A., Taracila, M. A., and Bonomo, R. A. (2011) Carbapenems: Past, present, and future. *Antimicrob. Agents Chemother. 55*, 4943−4960.

(2) Nicolau, D. P. (2008) Carbapenems: A potent class of antibiotics. *Expert Opin. Pharmacother. 9*, 23−37.

(3) Drawz, S. M., and Bonomo, R. A. (2010) Three decades of beta-lactamase inhibitors. *Clin. Microbiol. Rev. 23*, 160−201.

(4) Helfand, M. S., and Bonomo, R. A. (2003) Beta-lactamases: A survey of protein diversity. *Curr. Drug Targets: Infect. Disord. 3*, 9−23.

(5) Ambler, R. P., Coulson, A. F., Frere, J. M., Ghuysen, J. M., Joris, B., Forsman, M., Levesque, R. C., Tiraby, G., and Waley, S. G. (1991) A standard numbering scheme for the class A beta-lactamases. *Biochem. J. 276* (1), 269−270.

(6) Fisher, J. F., Meroueh, S. O., and Mobashery, S. (2005) Bacterial resistance to beta-lactam antibiotics: Compelling opportunism, compelling opportunity. *Chem. Rev. 105*, 395−424.

(7) Wilke, M. S., Lovering, A. L., and Strynadka, N. C. (2005) Beta-lactam antibiotic resistance: A current structural perspective. *Curr. Opin. Microbiol. 8*, 525−533.

(8) Fisher, J. F., and Mobashery, S. (2009) Three decades of the class A beta-lactamase acyl−enzyme. *Curr. Protein Pept. Sci. 10*, 401−407.

(9) Maveyraud, L., Mourey, L., Kotra, L. P., Pedelacq, J.-D., Guillet, V., Mobashery, S., and Samama, J. P. (1998) Structural basis for clinical longevity of carbapenem antibiotics in the face of challenge by the common class A beta-lactamases from antibiotic-resistant bacteria. *J. Am. Chem. Soc. 120*, 9748−9752.

(10) Tremblay, L. W., Fan, F., and Blanchard, J. S. (2010) Biochemical and structural characterization of *Mycobacterium tuberculosis* beta-lactamase with the carbapenems ertapenem and doripenem. *Biochemistry 49*, 3766−3773.

(11) Fonseca, F., Chudyk, E. I., van der Kamp, M. W., Correia, A., Mulholland, A. J., and Spencer, J. (2012) The basis for carbapenem hydrolysis by class A beta-lactamases: A combined investigation using crystallography and simulations. *J. Am. Chem. Soc. 134*, 18275−18285.

(12) Smith, C. A., Frase, H., Toth, M., Kumarasiri, M., Wiafe, K., Munoz, J., Mobashery, S., and Vakulenko, S. B. (2012) Structural basis for progression toward the carbapenemase activity in the GES family of beta-lactamases. *J. Am. Chem. Soc. 134*, 19512−19515.

(13) Poirel, L., Pitout, J. D., and Nordmann, P. (2007) Carbapenemases: Molecular diversity and clinical consequences. *Future Microbiol. 2*, 501−512.

(14) Walsh, T. R. (2008) Clinically significant carbapenemases: An update. *Curr. Opin. Infect. Dis. 21*, 367−371.

(15) Bush, K. (2010) Alarming beta-lactamase-mediated resistance in multidrug-resistant *Enterobacteriaceae*. *Curr. Opin. Microbiol. 13*, 558−564.

(16) Walsh, T. R. (2010) Emerging carbapenemases: A global perspective. *Int. J. Antimicrob. Agents 36* (Suppl. 3), S8−S14.

(17) Frase, H., Shi, Q., Testero, S. A., Mobashery, S., and Vakulenko, S. B. (2009) Mechanistic basis for the emergence of catalytic competence against carbapenem antibiotics by the GES family of beta-lactamases. *J. Biol. Chem. 284*, 29509−29513.

(18) Bebrone, C., Bogaerts, P., Delbruck, H., Bennink, S., Kupper, M. B., Rezende de Castro, R., Glupczynski, Y., and Hoffmann, K. M. (2013) GES-18, a new carbapenem-hydrolyzing GES-type beta-lactamase from *Pseudomonas aeruginosa* that contains Ile80 and Ser170 residues. *Antimicrob. Agents Chemother. 57*, 396−401.

(19) Frase, H., Toth, M., Champion, M. M., Antunes, N. T., and Vakulenko, S. B. (2011) Importance of position 170 in the inhibition of GES-type beta-lactamases by clavulanic acid. *Antimicrob. Agents Chemother. 55*, 1556−1562.

(20) Ke, W., Bethel, C. R., Thomson, J. M., Bonomo, R. A., and van den Akker, F. (2007) Crystal structure of KPC-2: Insights into carbapenemase activity in class A beta-lactamases. *Biochemistry 46*, 5732−5740.

(21) Petrella, S., Ziental-Gelus, N., Mayer, C., Renard, M., Jarlier, V., and Sougakoff, W. (2008) Genetic and structural insights into the dissemination potential of the extremely broad-spectrum class A beta-lactamase KPC-2 identified in an *Escherichia coli* strain and an *Enterobacter cloacae* strain isolated from the same patient in France. *Antimicrob. Agents Chemother. 52*, 3725−3736.

(22) Majiduddin, F. K., and Palzkill, T. (2003) Amino acid sequence requirements at residues 69 and 238 for the SME-1 beta-lactamase to confer resistance to beta-lactam antibiotics. *Antimicrob. Agents Chemother. 47*, 1062−1067.

(23) Chan, P. H., So, P. K., Ma, D. L., Zhao, Y., Lai, T. S., Chung, W. H., Chan, K. C., Yiu, K. F., Chan, H. W., Siu, F. M., Tsang, C. W., Leung, Y. C., and Wong, K. Y. (2008) Fluorophore-labeled beta-lactamase as a biosensor for beta-lactam antibiotics: A study of the biosensing process. *J. Am. Chem. Soc. 130*, 6351−6361.

(24) Wong, W. T., Au, H. W., Yap, H. K., Leung, Y. C., Wong, K. Y., and Zhao, Y. (2011) Structural studies of the mechanism for biosensing antibiotics in a fluorescein-labeled beta-lactamase. *BMC Struct. Biol. 11*, 15.

(25) Wong, W. T., Chan, K. C., So, P. K., Yap, H. K., Chung, W. H., Leung, Y. C., Wong, K. Y., and Zhao, Y. (2011) Increased structural flexibility at the active site of a fluorophore-conjugated beta-lactamase distinctively impacts its binding toward diverse cephalosporin antibiotics. *J. Biol. Chem. 286*, 31771−31780.

(26) Leslie, A. G. (2006) The integration of macromolecular diffraction data. *Acta Crystallogr., Sect. D: Biol. Crystallogr. 62*, 48−57.

(27) Evans, P. (2006) Scaling and assessment of data quality. *Acta Crystallogr., Sect. D: Biol. Crystallogr. 62*, 72−82.

(28) McCoy, A. J. (2007) Solving structures of protein complexes by molecular replacement with Phaser. *Acta Crystallogr., Sect. D: Biol. Crystallogr. 63*, 32−41.

(29) Murshudov, G. N., Vagin, A. A., and Dodson, E. J. (1997) Refinement of macromolecular structures by the maximum-likelihood method. *Acta Crystallogr., Sect. D: Biol. Crystallogr. 53*, 240−255.

(30) Emsley, P., and Cowtan, K. (2004) Coot: Model-building tools for molecular graphics. *Acta Crystallogr., Sect. D: Biol. Crystallogr. 60*, 2126−2132.

(31) Potterton, L., McNicholas, S., Krissinel, E., Gruber, J., Cowtan, K., Emsley, P., Murshudov, G. N., Cohen, S., Perrakis, A., and Noble, M. (2004) Developments in the CCP4 molecular−graphics project. *Acta Crystallogr., Sect. D: Biol. Crystallogr. 60*, 2288−2294.

(32) Chen, C. C., and Herzberg, O. (2001) Structures of the acyl−enzyme complexes of the *Staphylococcus aureus* beta-lactamase mutant Glu166Asp:Asn170Gln with benzylpenicillin and cephaloridine. *Biochemistry 40*, 2351−2358.

(33) Schneider, K. D., Ortega, C. J., Renck, N. A., Bonomo, R. A., Powers, R. A., and Leonard, D. A. (2011) Structures of the class D carbapenemase OXA-24 from *Acinetobacter baumannii* in complex with doripenem. *J. Mol. Biol. 406*, 583−594.